

Supplementary Online Content

Pizzagalli DA, Webb CA, Dillon DG, et al. Pretreatment rostral anterior cingulate cortex theta activity in relation to symptom improvement in depression: a randomized clinical trial. *JAMA Psychiatry*. Published online April 11, 2018.
doi:10.1001/jamapsychiatry.2018.0252

eMethods. Expanded Methodology

eResults. Expanded Results

eDiscussion. Expanded Discussion

eFigure 1. Location of the A Priori Rostral Anterior Cingulate Cortex Region of Interest Used for the Analyses

eFigure 2. Scatterplots Displaying the Significant Association Between Resting rACC Theta Activity at Baseline and One Week Later for the Sertraline and Placebo Groups

eTable 1. Coordinates and Brodmann Areas of the Voxels Included in the rACC Regions-of-Interest Used for the Current Analyses

eTable 2. Summary of Dropout Rates for the Sertraline and Placebo Groups

eAppendix. Author Contributions

This supplementary material has been provided by the authors to give readers additional information about their work.

eMethods. Expanded Methodology

Sample size and power analyses for the clinical trial

The sample size of $n=300$ was determined to allow sufficient power (at least 80%) of a significance test with $\alpha=.05$ two-sided, to detect interaction effects of multiple (about 40) potential moderators of the treatment effect on the primary outcome, after adjusting for multiple testing. The postulated effect sizes¹⁻³ of the moderators were 0.15 - 0.2.

Methods used to generate the random allocation sequence

The randomization was stratified by site, depression symptom severity, and chronicity. Within each stratum, block randomization with random block size of 2 or 4 was implemented through a commercial clinical trial data managing software StudyTrax. When a site coordinator provided information about all study inclusion/exclusion criteria for a patient, the software checked for eligibility and if the patient was eligible the software provided a randomization assignment, which was directly communicated to the site pharmacist.

Exclusion criteria

In addition to the exclusion criteria mentioned in the main text, participants were excluded when any of the following criteria were met: 1) current pregnancy, breastfeeding, no use of contraception; 2) lifetime history of psychosis or bipolar disorder; 3) substance dependence in the past six months or substance abuse in the past two months; 4) unstable psychiatric or general medical conditions requiring hospitalization; 5) study medication contraindication; 6) clinically significant laboratory abnormalities; 7) history of epilepsy or condition requiring an anticonvulsant; 8) electroconvulsive therapy (ECT), vagal nerve

stimulation (VNS), transcranial magnetic stimulation (TMS) or other somatic treatments in the current episode; 9) medications (including but not limited to antipsychotics and mood stabilizers); 10) current psychotherapy; 11) significant suicide risk; or (12) failure to respond to any antidepressant at adequate dose and duration in the current episode.

Participant compensation

Eligible participants received \$150 for completing the detailed interview and questionnaires administered at the screening session and \$68 for the two EEG sessions. They also received the following compensation for other components not presented here: up to \$200 for two MRI sessions, up to \$32 in earnings in a behavioral task, \$25 to complete blood samples for research purposes (up to \$175 total), \$50 for genetic blood sampling, and \$50 for completing the final clinical rating session of the study. The total possible compensation was \$725.

Participants were not compensated for the follow-up visits.

Participants lost to follow-up

Of the 143 participants who received sertraline, 117 completed the 8-week intervention and 26 discontinued (7 lost to follow-up). Of the 144 participants who received placebo, 125 completed the 8-week intervention and 19 discontinued (5 lost to follow-up). For a detailed summary of reasons for discontinuing the study for each group, see Supplementary Table 2.

EEG acquisition setup

Resting EEG was recorded during four 2-minute periods (4 min: eyes-closed (C); 4 min: eyes open (O)) in a counterbalanced order (COOC or OCCO). Participants were instructed to

remain still and minimize blinks or eye movements, and to fixate on a centrally presented cross during the eyes-open condition.

For participants recruited through Massachusetts General Hospital, EEG data were collected at McLean Hospital. At Columbia University College of Physicians & Surgeons, 72-channel EEG were collected using a 24-bit BioSemi system (sampling rate: 256 Hz, bandpass: DC-251.3 Hz), a Lycra stretch electrode cap (Electro-Cap International Inc., Ohio), and an active reference (ActiveTwo EEG system) at electrode locations PPO1 (common mode sense) and PPO2 (driven right leg). At McLean Hospital, 129-channel EEG data were collected using a Geodesic Net system (sampling rate: 250 Hz, bandpass: 0.01-100 Hz), with Cz as reference (Electrical Geodesics Inc., Oregon). At the University of Michigan, 60-channel EEG data were collected using the 32-bit NeuroScan Synamp (Compumedics, TX) system (sampling rate: 250 Hz, bandpass: 0.5-100 Hz), a Lycra stretch electrode cap, and a nose reference. Finally, at the University of Texas, 62-channel EEG data were recorded (sampling rate: 250 Hz, bandpass: DC-100 Hz) using a 32-bit NeuroScan Synamp system, a Lycra stretch electrode cap, and a nose reference. At all sites, amplifier calibrations were performed.

Experimenters were certified by the Columbia EEG team (Drs. Tenke, Kayser, Bruder) after demonstrating accurate EEG cap placement and delivery of task instructions via video conference, and then submitting satisfactory EEG data from a pilot subject.

EEG preprocessing

To minimize cross-site differences, a standardized analysis pipeline was developed and executed by the Columbia site (see ⁴ for details). Briefly, a common montage was created to allow integration of data across all sites, and electrodes with poor signal were interpolated using

spherical splines.⁵ Recordings with more than 20% unusable data were dropped. Next, a spatial principal component analysis approach⁶ was used to correct for blink artifacts. Blink-free EEG data were then segmented into non-overlapping 2-s epochs and band-passed at 1-60 Hz (24 dB/octave). Residual artifacts (e.g., amplifier drift, movement-related artifacts) were identified on a channel-by-channel and trial-by-trial (epoch-by-epoch) basis⁷, and flagged epochs were interpolated using spherical spline from data of all valid channels for a given epoch. No differences emerged with respect to the number of artifact-free, 2-sec EEG epochs available for source localization analyses (mean \pm SD: Columbia: 92.6 ± 3.1 ; McLean: 87.9 ± 3.3 ; University of Texas: 86.5 ± 5.9 ; University of Michigan: 84.2 ± 12.1). Of the 266 subjects with EEG recordings, 248 (93%) had usable EEG data for analyses. The 18 subjects with unusable EEG recordings were primarily attributable to too many bad EEG channels.

Low Resolution Electromagnetic Tomography (LORETA): Processing steps, assumptions and cross-modal validation

LORETA steps: LORETA analyses were conducted at the McLean Hospital site, blind to randomization arm and clinical outcome. First, a discrete Fourier transform was applied to the scalp EEG data for a narrow (6.5-8.0 Hz) and broader (4.5-7 Hz) theta band. Second, LORETA was used to compute current density (i.e., the amount of electrical current flowing through a solid; unit: amperes per square meter, A/m^2) as the linear, weighted sum of the scalp electrical potentials, which was squared to obtain power of current density for each voxel. Third, LORETA data were normalized so that, for each frequency band separately, the total current density across all voxels equaled 1, and were then log-transformed to normalize their distribution. Finally, theta current density was extracted from the rACC cluster (14 voxels; Supplement Figure 1 and

Supplement Table 1) previously associated with better antidepressant outcome.⁸ This cluster was also used by ref.⁹ and spatially overlapped with the one linked to treatment outcome in two additional EEG studies.^{10,11} For comparability with all prior EEG studies in this area (e.g.,⁸⁻¹¹), the original LORETA algorithm was used (number of voxels: 2394; voxel dimension: 7 mm³).

Assumptions: LORETA¹² is a form of Laplacian-weighted minimal norm solution that solves the inverse problem without postulating a specified number of sources by making two assumptions: (i) neighboring neurons are synchronously activated; and (ii) scalp-recorded EEG originates mostly from cortical gray matter. The first assumption is implemented by computing the “smoothest” of all possible activity distributions (i.e., the solution with the smoothest spatial distribution) by minimizing the Laplacian (i.e., the second spatial derivatives) of the current sources. The second assumption is implemented by constraining the solution space to cortical gray matter (and hippocampi), as defined by a brain template from the Montreal Neurological Institute (MNI). For the current study, we used the LORETA version that implements a three-shell spherical head model registered to the Talairach brain atlas (available as digitized MRI from the Brain Imaging Centre, Montreal Neurological Institute¹³) and EEG electrode coordinates derived from cross-registrations between spherical and realistic head geometry.¹⁴ The solution space (2,394 voxels; voxel dimensions: 7x7x7 mm) is limited to cortical gray matter and hippocampi, as defined by a digitized probability atlas provided by the MNI.

Cross-modal validation of LORETA: Validation for the LORETA algorithm comes from various sources. First, physiologically meaningful findings that mirror data from functional magnetic resonance imaging (fMRI) or positron emission tomography (PET) studies have emerged for basic visual, auditory, motor and cognitive tasks (e.g.,¹⁵⁻¹⁸) and epileptic discharges (e.g.,^{19,20}). Second, validation emerged from studies directly combining LORETA with

functional fMRI^{21,22}, structural MRI^{23,24}, PET²⁵, but see ²⁶, and intracranial recordings^{27,28}, with localization deviations from fMRI loci of 16 mm²¹ and 14.5 mm²², which is in the range of the spatial resolution of LORETA (~1-2 cm). Finally, and directly relevant to the current analyses, a prior concurrent EEG-PET study provided evidence that rACC theta activity (extracted from the identical cluster as used in the current study) was positively correlated with glucose metabolism from the same region.²⁹ These cross-modal findings indicate that EEG and PET findings linking rACC function and outcome in MDD might reflect similar processes.

Spatial smoothing. To minimize potential site differences, LORETA data were computed using three degrees of spatial smoothing: no extra smoothing, intermediate over-smoothing, and large smoothing. The key findings were replicated with no extra smoothing and use of a narrower theta frequency range (see *Supplemental Results*).

Theta band definition: To evaluate the robustness of the findings, analyses were performed using both a narrow (6.5-8.0 Hz) and broader (4.5-7 Hz) theta band. This choice was also motivated by the fact that prior studies on this topic have used different definitions of the theta band, including 6.5-8 Hz,^{8,10} 4-7 Hz,⁹ and 4.5-7.5 Hz.¹¹

Predictor selection

Given the relatively large number of terms, we used a step-wise procedure to pare down the number of predictors in our model.³⁰ In Step 1, all predictors were included. In Step 2, we retained those predictors from Step 1 significant at $p < .20$. In Step 3, we retained those predictors from Step 2 with $ps < .10$. Finally, in Step 4, we retained those predictors from Step 3 with $ps < .05$. To the extent that a significant rACC theta finding emerged (i.e., remained significant in Step 4), we also tested whether the inclusion of this rACC theta term in our model yielded

significantly improved fit relative to a “reduced” model (i.e., including all predictors from the final model, but excluding the rACC theta term).

eResults. Expanded Results

In the main text, we noted that the final baseline model accounted for 39.6% of the between-subjects variance in the slope of symptom improvement (38.2% for Week 1 rACC theta model). Similar to ref.³⁰, these values were estimated by comparing the covariance parameter estimates (from the HLM output) representing the total variance in the slope of change across subjects from an *unconditional growth model* (i.e., where *Time* is the only predictor in the model) relative to the residual variance in the slope of change from the final (Step 4) model. (For additional details, see ref.³¹, in particular equation 4.14).

Test-retest reliability

In the main text we note that baseline and Week 1 rACC theta exhibited acceptable test-retest reliability in both the sertraline ($r=0.70$; $p<1\times 10^{-4}$; Supplemental Figure 2A) and placebo ($r=0.64$; $p<1\times 10^{-4}$; Supplemental Figure 2B) groups. However, in response to a reviewer’s suggestion, we also tested a *Group* (SSRI vs. Placebo) x *Time* (Baseline, Week 1) interaction, which was non-significant ($F(1,233)=0.00$, $p=.95$), indicating no group differences in rACC theta activity over time.

Completer analyses

The final model was re-run excluding those patients who dropped out of treatment prior to the Week 8 HRSD assessment ($n=34$). Higher baseline rACC theta activity (4.5-7Hz) remained significantly associated with depressive symptom improvement (intercept:

t(202)=-2.95, p=.004, b=-6.61, 95% CI, -11.03 to -2.20); slope: t(207)=-2.88, p=.004, b=-1.04, 95% CI, -1.76 to -0.33). The corresponding analyses with Week 1 data yielded significant findings for the intercept (t(194)=-2.04, p=.043, b=-4.92, 95% CI, -9.68 to -0.15) but a nonsignificant trend for the slope (t(198)=-1.85, p=0.07, b=-0.73, 95% CI, -1.51 to 0.50).

Analyses using different theta frequency definition and spatial smoothing

Analyses described in the main text were based on theta activity defined as 4.5-7 Hz, and while applying an intermediate smoothing parameter to LORETA data. Other LORETA studies have defined theta activity as 6.5-8 Hz and applied no extra smoothing (e.g.,⁸). Accordingly, we re-ran our final models from our intent-to-treat and completer analyses with the narrower theta range (6.5-7 Hz) and with no extra smoothing. A similar pattern of findings emerged for our intent-to-treat sample for both baseline and the Week 1 EEG assessments (all $|t_s| > 1.99$ and $p_s < .05$), although findings were less consistent with the completer sample [baseline rACC theta effect at intercept: t(204)=-2.26, p=.03, b=-5.41, 95% CI, -10.13 to -0.70; slope: t(209)=-1.96, p=.05, b=-0.76, 95% CI, -1.53 to 0.003; Week 1 rACC theta effect at intercept: t(197)=-1.63, p=.10, b=-3.98, 95% CI, -8.78 to 0.83; slope: t(199)=-1.49, p=.14, b=-0.59, 95% CI, -1.38 to 0.19].

Exploratory analyses of trending *Group x rACC theta x Time* interaction for week 1

As reported in the main text, the *Treatment Group x rACC theta x Time* interaction was not significant for either baseline [t(217)=0.45, p=.65, b=0.32, 95% CI: -1.08 to 1.72] or Week 1 [t(210)=1.76, p=.08, b=1.36, 95% CI: -0.16 to 2.88] rACC theta (intent-to-treat analyses). At the request of an anonymous reviewer, we explored the trending *Treatment Group x rACC theta x*

Time interaction for the Week 1 data, which revealed that at relatively lower levels of (Week 1) rACC theta there was greater improvement in SSRI than placebo, in comparison to those with higher levels of rACC theta where the between-group difference in symptom improvement was smaller. It is important to note that there are two relevant interaction terms that test whether treatment group moderates rACC-outcome associations: the *Treatment Group x rACC theta* effect at the intercept (time centered to represent estimated post-treatment HRSD scores) and on the linear slope estimates (captured by the *Treatment Group x rACC theta x Time* interaction). Moreover, these two interactions can be tested for both baseline rACC theta and Week 1 rACC theta, resulting in 4 interaction tests in total. In the end, all 4 of these effects are nonsignificant (for baseline rACC theta: effect on the intercept [t(222)=-0.02, p=.99, b=-0.07, 95% CI: -8.56 to 8.41] and on the linear slope estimates [t(217)=0.45, p=.65, b=0.32, 95% CI: -1.08 to 1.72]; for Week 1 rACC theta: effect on the intercept [t(212)=1.58, p=.12, b=7.31, 95% CI: -1.82 to 16.44] and on the linear slope estimates [t(210)=1.76, p=.08, b=1.36, 95% CI: -0.16 to 2.88]. For these reasons, although we describe these effects in the Supplement, we chose not to interpret or discuss in the main text the 1 out of 4 tests which was a nonsignificant trend.

Association with baseline characteristics

At the request of an anonymous reviewer, we tested the association between rACC theta activity and a range of relevant baseline patient characteristics. A significant inverse association emerged between age and rACC theta at both baseline ($r=-.23$; $p<.01$) and Week 1 ($r=-.25$; $p<.01$). Associations were not significant when testing other baseline characteristics, including depressive symptom severity, anxiety severity, anhedonia severity, and years of education (all $ps>.18$). In response to an additional request from an anonymous reviewer, we also tested

whether the estimated number of previous major depressive episodes (MDEs) or receiving medication treatment since the onset of the current episode was related to rACC levels. Neither the number of previous MDEs ($p=.09$) or medication treatment ($p=.11$) correlated with rACC theta levels, nor moderated rACC theta-outcome associations (all $ps>.19$).

Prediction model removing clinical and demographic covariates

At the request of an anonymous reviewer, an additional control analysis was performed by removing all clinical and demographic characteristics. Accordingly, we re-ran our baseline and Week 1 rACC final models removing these model terms. The same pattern of findings emerged with rACC theta activity significantly predicting depressive symptom improvement. Specifically, higher baseline rACC theta emerged as a significant predictor of lower Week 8 HRSD scores [i.e., significant effect on the intercept: $t(229)=-3.04$, $p=.003$, $b=-7.12$, 95% CI: -11.73 to -2.50] and greater depressive symptom improvement [i.e., significant effect on slope estimates: $t(225)=-3.47$, $p<.001$, $b=-1.31$, 95% CI: -2.05 to -0.56]. For Week 1 rACC theta, these corresponding effects were also both significant [$t(218)=-2.78$, $p=.006$, $b=-6.97$, 95% CI: -11.93 to -2.03 and $t(217)=-2.08$, $p=.040$, $b=-0.86$, 95% CI: -1.67 to -0.04, respectively].

Prediction model examining rACC alpha power

In prior EEG studies on this topic, theta activity in the rACC emerged as the most replicated finding.^{8,10,11,32} Critically, in the first study to test the relation between rACC theta activity and outcome, Pizzagalli et al.⁸ tested seven frequency bands (from the delta to high beta band) and the rACC-outcome findings were specific to theta. This specificity had been expected in light of independent literature (1) linking rACC activity and treatment response³³ and (2)

highlighting the rACC as a generator of theta activity in both rodents and humans.³⁴⁻³⁶ These independent lines of evidence justified our *a priori* hypotheses focused on the theta band, which also limited the number of statistical tests.

Given alpha-related abnormalities in MDD reported in the literature, an anonymous reviewer requested analyses testing whether alpha power localized to the rACC would predict treatment outcome. For lower alpha (8.5-10 Hz), higher baseline rACC alpha activity emerged as a significant predictor of lower Week 8 HRSD scores [i.e., significant effect on the intercept: $t(226)=-2.26$, $p=.025$, $b=-4.41$, 95% CI: -8.26 to -0.56] but not greater depressive symptom improvement [i.e., non-significant effect on slope estimates: $t(221)=-1.91$, $p=.06$, $b=-0.62$, 95% CI: -1.26 to 0.02]. The latter two effects were both non-significant (both $ps>.81$) when controlling for corresponding rACC theta activity (whereas both theta effects remained significant [both $ps<.04$] when controlling for rACC (lower) alpha activity). For higher alpha (10.5-12 Hz) activity, neither effect was significant (both $ps>.20$).

eDiscussion. Expanded Discussion

As discussed in the main text, links between increased pretreatment theta activity in the rACC have been replicated in several studies using LORETA.^{8-11; but see 37} These replications contrast with inconsistent findings emerging from studies evaluating scalp frontal theta power (for review, see^{38,39}). For example, *decreased* pretreatment theta band activity predicted response to tricyclic antidepressants, imipramine and SSRIs.^{40,41} In contrast, *increased* pre-treatment theta power was found to differentiate paroxetine responders from non-responders.⁴² Similarly, increased pre-treatment theta power predicted better treatment response to a variety of antidepressants.⁴³ The reasons for these opposite patterns are unclear. Collectively, these findings

indicate that source-localized rACC theta current density might represent a more reliable prognostic predictor of treatment outcome.

eReferences.

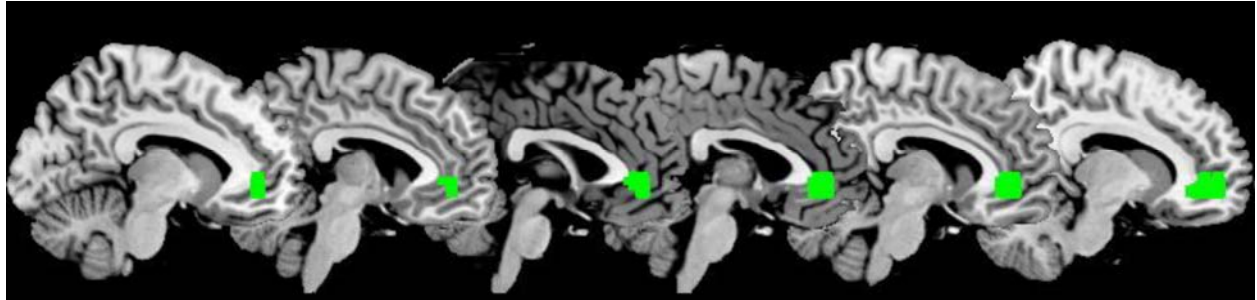
1. Petkova E, Ogden RT, Tarpey T, Ciarleglio A, Jiang B, Su Z, Carmody T, Adams P, Kraemer HC, Grannemann BD, Oquendo MA, Parsey R, Weissman M, McGrath PJ, Fava M, Trivedi MH. Statistical Analysis Plan for Stage 1 EMBARC (Establishing Moderators and Biosignatures of Antidepressant Response for Clinical Care) Study. *Contemp Clin Trials Commun.* 2017;6:22-30.
2. Trivedi MH, McGrath PJ, Fava M, Parsey RV, Kurian BT, Phillips ML, Oquendo MA, Bruder G, Pizzagalli D, Toups M, Cooper C, Adams P, Weyandt S, Morris DW, Grannemann BD, Ogden RT, Buckner R, McInnis M, Kraemer HC, Petkova E, Carmody TJ, Weissman MM. Establishing moderators and biosignatures of antidepressant response in clinical care (EMBARC): Rationale and design. *J Psychiatr Res.* 2016;78.
3. Kraemer HC. Discovering, comparing, and combining moderators of treatment on outcome after randomized clinical trials: a parametric approach. *Stat Med.* 2013;32(11):1964-1973.
4. Tenke CE, Kayser J, Pechtel P, Webb CA, Dillon DG, Goer F, Murray L, Deldin P, Kurian BT, McGrath PJ, Parsey R, Trivedi M, Fava M, Weissman MM, McInnis M, Abraham K, E. Alvarenga J, Alschuler DM, Cooper C, Pizzagalli DA, Bruder GE. Demonstrating test-retest reliability of electrophysiological measures for healthy adults in a multisite study of biomarkers of antidepressant treatment response. *Psychophysiology.* 2017;54(1):34-50.
5. Perrin F, Pernier J, Bertrand O, Echallier JF. Spherical splines for scalp potential and current density mapping. *Electroencephalogr Clin Neurophysiol.* 1989;72(2):184-187.
6. NeuroScan I. *SCAN 4.3 - Vol. II. EDIT 4.3 - Offline Analysis of Acquired Data (Document Number 2203, Revision D).* El Paso, TX.; 2003.
7. Kayser J, Tenke CE. Electrical distance as a reference-free measure for identifying artifacts in multichannel electroencephalogram (EEG) recordings. *Psychophysiology.* 2006;43:S51.
8. Pizzagalli D, Pascual-Marqui RD, Nitschke JB, Oakes TR, Larson CL, Abercrombie HC, Schaefer SM, Koger J V., Benca RM, Davidson RJ. Anterior cingulate activity as a predictor of degree of treatment response in major depression: Evidence from brain electrical tomography analysis. *Am J Psychiatry.* 2001;158(3):405-415.
9. Korb AS, Hunter AM, Cook IA, Leuchter AF. Rostral anterior cingulate cortex theta current density and response to antidepressants and placebo in major depression. *Clin Neurophysiol.* 2009;120(7):1313-1319.
10. Mulert C, Juckel G, Brunmeier M, Karch S, Leicht G, Mergl R, Möller H-J, Hegerl U, Pogarell O. Prediction of treatment response in major depression: Integration of concepts. *J Affect Disord.* 2007;98(3):215-225.
11. Rentzsch J, Adli M, Wiethoff K, Gómez-Carrillo de Castro A, Gallinat J. Pretreatment anterior cingulate activity predicts antidepressant treatment response in major depressive episodes. *Eur Arch Psychiatry Clin Neurosci.* 2014;264(3):213-223.
12. Pascual-Marqui RD, Lehmann D, Koenig T, Kochi K, Merlo MC, Hell D, Koukkou M. Low resolution brain electromagnetic tomography (LORETA) functional imaging in acute, neuroleptic-naive, first-episode, productive schizophrenia. *Psychiatry Res.* 1999;90(3):169-179.
13. Evans, A. C., Collins, D. L., Mills, S. R., Brown, E. D., Kelly, R. L., & Peters TM. 3D

- statistical neuroanatomical models from 305 MRI volumes. *Proc IEEE Nucl Sci Symp Med Imaging Conf.* 1993;95:1813-1817.
14. Towle VL, Bolaños J, Suarez D, Tan K, Grzeszczuk R, Levin DN, Cakmur R, Frank SA, Spire JP. The spatial location of EEG electrodes: locating the best-fitting sphere relative to cortical anatomy. *Electroencephalogr Clin Neurophysiol.* 1993;86(1):1-6.
 15. Mulert C, Gallinat J, Pascual-Marqui R, Dorn H, Frick K, Schlattmann P, Mientus S, Herrmann WM, Winterer G. Reduced Event-Related Current Density in the Anterior Cingulate Cortex in Schizophrenia. *Neuroimage.* 2001;13(4):589-600.
 16. Pizzagalli DA, Lehmann D, Hendrick AM, REGARD M, Pascual-Marqui RD, Davidson RJ. Affective judgments of faces modulate early activity (approximately 160 ms) within the fusiform gyri. *Neuroimage.* 2002;16(3 Pt 1):663-677.
 17. Thut G, Hauert CA, Morand S, Seeck M, Landis T, Michel C. Evidence for interhemispheric motor-level transfer in a simple reaction time task: an EEG study. *Exp Brain Res.* 1999;128(1-2):256-261.
 18. Whittingstall K, Bartels A, Singh V, Kwon S, Logothetis NK. Integration of EEG source imaging and fMRI during continuous viewing of natural movies. *Magn Reson Imaging.* 2010;28(8):1135-1142.
 19. Lantz G, Michel CM, Pascual-Marqui RD, Spinelli L, Seeck M, Seri S, Landis T, Rosen I. Extracranial localization of intracranial interictal epileptiform activity using LORETA (low resolution electromagnetic tomography). *Electroencephalogr Clin Neurophysiol.* 1997;102(5):414-422.
 20. Strobbe G, Carrette E, López JD, Montes Restrepo V, Van Roost D, Meurs A, Vonck K, Boon P, Vandenberghe S, van Mierlo P. Electrical source imaging of interictal spikes using multiple sparse volumetric priors for presurgical epileptogenic focus localization. *NeuroImage Clin.* 2016;11:252-263.
 21. Mulert C, Jäger L, Schmitt R, Bussfeld P, Pogarell O, Möller H-J, Juckel G, Hegerl U. Integration of fMRI and simultaneous EEG: towards a comprehensive understanding of localization and time-course of brain activity in target detection. *Neuroimage.* 2004;22(1):83-94.
 22. Vitacco D, Brandeis D, Pascual-Marqui R, Martin E. Correspondence of event-related potential tomography and functional magnetic resonance imaging during language processing. *Hum Brain Mapp.* 2002;17(1):4-12.
 23. Worrell GA, Lagerlund TD, Sharbrough FW, Brinkmann BH, Busacker NE, Cicora KM, O'Brien TJ. Localization of the epileptic focus by low-resolution electromagnetic tomography in patients with a lesion demonstrated by MRI. *Brain Topogr.* 2000;12(4):273-282.
 24. Akdeniz G. Electrical source localization by LORETA in patients with epilepsy: Confirmation by postoperative MRI. *Ann Indian Acad Neurol.* 2016;19(1):37.
 25. Pizzagalli DA, Oakes TR, Fox AS, Chung MK, Larson CL, Abercrombie HC, Schaefer SM, Benca RM, Davidson RJ. Functional but not structural subgenual prefrontal cortex abnormalities in melancholia. *Mol Psychiatry.* 2004;9(4):325,393-405.
 26. Gamma A, Lehmann D, Frei E, Iwata K, Pascual-Marqui RD, Vollenweider FX. Comparison of simultaneously recorded [H₂(15)O]-PET and LORETA during cognitive and pharmacological activation. *Hum Brain Mapp.* 2004;22(2):83-96.
 27. Seeck M, Lazeyras F, Michel CM, Blanke O, Gericke CA, Ives J, Delavelle J, Golay X, Haenggeli CA, de Tribolet N, Landis T. Non-invasive epileptic focus localization using

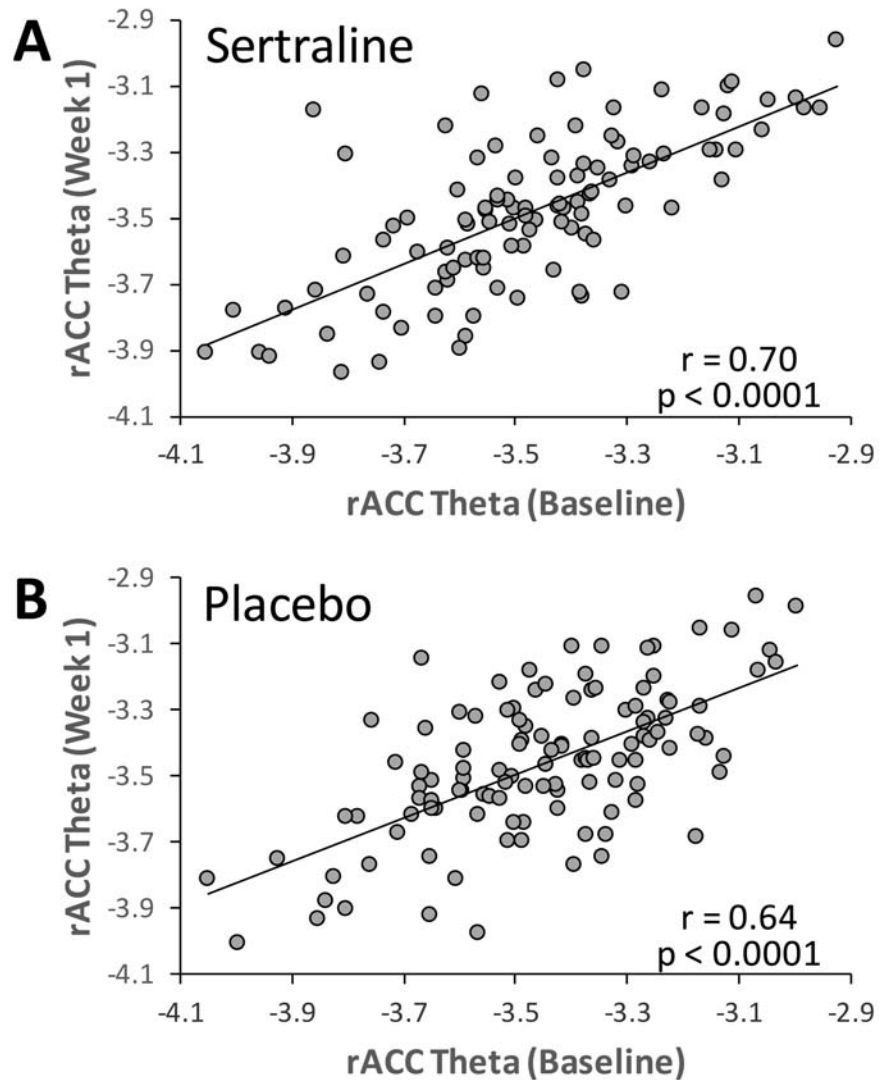
- EEG-triggered functional MRI and electromagnetic tomography. *Electroencephalogr Clin Neurophysiol*. 1998;106(6):508-512.
28. Grova C, Aiguabella M, Zelmann R, Lina J-M, Hall JA, Kobayashi E. Intracranial EEG potentials estimated from MEG sources: A new approach to correlate MEG and iEEG data in epilepsy. *Hum Brain Mapp*. 2016;37(5):1661-1683.
 29. Pizzagalli DA, Oakes TR, Davidson RJ. Coupling of theta activity and glucose metabolism in the human rostral anterior cingulate cortex: an EEG/PET study of normal and depressed subjects. *Psychophysiology*. 2003;40(6):939-949.
 30. Fournier JC, DeRubeis RJ, Shelton RC, Hollon SD, Amsterdam JD, Gallop R. Prediction of response to medication and cognitive therapy in the treatment of moderate to severe depression. *J Consult Clin Psychol*. 2009;77(4):775-787.
 31. Singer JD, Willett JB. *Applied Longitudinal Data Analysis: Modeling Change and Event Occurrence*. Oxford University Press, New York; 2003.
 32. Korb AS, Hunter AM, Cook IA, Leuchter AF. Rostral Anterior Cingulate Cortex Theta Current Density and Response to Antidepressants and Placebo in Major Depression. *Clin Neurophysiol*. 2009;120(7):1313-1319.
 33. Mayberg HS, Brannan SK, Mahurin RK, Jerabek PA, Brickman JS, Tekell JL, Silva JA, McGinnis S, Glass TG, Martin CC, Fox PT. Cingulate function in depression: a potential predictor of treatment response. [Miscellaneous Article]. *Neuroreport*. 1997;8(4):1057-1061.
 34. Asada H, Fukuda Y, Tsunoda S, Yamaguchi M, Tonoike M. Frontal midline theta rhythms reflect alternative activation of prefrontal cortex and anterior cingulate cortex in humans. *Neurosci Lett*. 1999;274(1):29-32.
 35. Feenstra BWA, Holsheimer J. Dipole-like neuronal sources of theta rhythm in dorsal hippocampus, dentate gyrus and cingulate cortex of the urethane-anesthetized rat. *Electroencephalogr Clin Neurophysiol*. 1979;47(5):532-538.
 36. Holsheimer J. Generation of theta activity (RSA) in the cingulate cortex of the rat. *Exp Brain Res*. 1982;47(2):309-312.
 37. Arns M, Etkin A, Hegerl U, Williams LM, DeBattista C, Palmer DM, Fitzgerald PB, Harris A, deBeuss R, Gordon E. Frontal and rostral anterior cingulate (rACC) theta EEG in depression: Implications for treatment outcome? *Eur Neuropsychopharmacol*. 2015;25(8):1190-1200.
 38. Baskaran A, Milev R, McIntyre RS. The neurobiology of the EEG biomarker as a predictor of treatment response in depression. *Neuropharmacology*. 2012;63(4):507-513.
 39. Iosifescu DV. Electroencephalography-Derived Biomarkers of Antidepressant Response. *Harv Rev Psychiatry*. 2011;19(3):144-154.
 40. Iosifescu D V., Greenwald S, Devlin P, Mischoulon D, Denninger JW, Alpert JE, Fava M. Frontal EEG predictors of treatment outcome in major depressive disorder. *Eur Neuropsychopharmacol*. 2009;19(11):772-777.
 41. Knott VJ, Telner JJ, Lapierre YD, Browne M, Horn ER. Quantitative EEG in the prediction of antidepressant response to imipramine. *J Affect Disord*. 1996;39(3):175-184.
 42. Knott V, Mahoney C, Kennedy S, Evans K. Pre-Treatment EEG and It's Relationship to Depression Severity and Paroxetine Treatment Outcome. *Pharmacopsychiatry*. 2000;33(6):201-205.

43. Spronk D, Arns M, Barnett KJ, Cooper NJ, Gordon E. An investigation of EEG, genetic and cognitive markers of treatment response to antidepressant medication in patients with major depressive disorder: a pilot study. *J Affect Disord*. 2011;128(1-2):41-48.

eFigure 1. Location of the *A Priori* Rostral Anterior Cingulate Cortex (rACC) Region of Interest (See Green Cluster) Used for the Analyses.



eFigure 2. Scatterplots Displaying the Significant Association Between Resting rACC Theta Activity at Baseline and One Week Later for the Sertraline and Placebo Groups.



eTable 1. Coordinates (in mm, origin at anterior commissure) and Brodmann Areas of the Voxels Included in the rACC Regions-of-Interest Used for the Current Analyses. This identical ROI has been used by ref. ⁸ and ⁹, and spatially overlapped with rACC clusters emerging from additional studies in this area.^{10,11}

X=left(-) to right(+); Y=posterior(-) to anterior(+); Z=inferior(-) to superior(+).

X	Y	Z	Brodman area	Region	Side
11	45	-6	BA32	Anterior Cingulate Cortex	Right
11	38	-6	BA10	Medial Frontal Gyrus	Right
4	45	-6	BA32	Anterior Cingulate Cortex	Right
11	52	-6	BA32	Anterior Cingulate Cortex	Right
4	38	1	BA24	Anterior Cingulate Cortex	Right
-3	38	1	BA24	Anterior Cingulate Cortex	Left
4	45	1	BA32	Anterior Cingulate Cortex	Right
11	45	1	BA10	Anterior Cingulate Cortex	Right
-3	45	-6	BA32	Anterior Cingulate Cortex	Left
4	38	-6	BA32	Anterior Cingulate Cortex	Right
-3	45	1	BA32	Anterior Cingulate Cortex	Left
11	52	1	BA10	Medial Frontal Gyrus	Right
-10	45	-6	BA32	Anterior Cingulate Cortex	Left
-10	45	1	BA10	Anterior Cingulate Cortex	Left

eTable 2. Summary of Dropout Rates for the Sertraline and Placebo Groups.

Discontinued Sertraline (n = 26)	Discontinued Placebo (n = 19)
- Lost to follow-up (n=7)	- Lost to follow-up (n=5)
- Non-adherent (n=6)	- Non-adherent (n=6)
- Wanted to discontinue medication (n=3)	- Wanted to discontinued Medication (n=4)
- Believed treatment not working (n=1)	- Believed treatment not working (n=2)
- Side effects unacceptable (n=9)	- Side effects unacceptable (n=1)
- Found study too burdensome (n=3)	- Moved from area (n=1)
- Developed medical condition (n=1)	- Became pregnant (n=1)
- Became danger to self (n=1)	- Other (n=6)
- Hospitalized for worsening depression (n=1)	
- Hospitalized for suicidal ideation (n=1)	
- Other (n=4)	

Note: Numbers add up to more than the totals because participants discontinued for more than one reason

eAppendix. Author Contributions

Drs Pizzagalli and Webb served as co-first authors and contributed equally to the work. Each had full access to all of the data in the study and take responsibility for the integrity of the data and the accuracy of the data analysis.